

Andreev Spectroscopy Study of Multigap Pairing in PrOs₄Sb₁₂

C.S. TUREL¹, J.Y.T. WEI¹, W.M. YUHASZ², R. BAUMBACH² and M.B. MAPLE²

¹*Department of Physics, University of Toronto, 60 St. George Street, Toronto ON M5S-1A7 Canada*

²*Department of Physics and Institute for Pure and Applied Physical Sciences, University of California, San Diego, La Jolla, CA 92093 USA*

Experimental studies of the skutterudite superconductor PrOs₄Sb₁₂ have reported various field-vs-temperature phase diagrams, with mixed evidence for nodes in the pairing gap. Some experiments have also indicated the presence of multiple gaps, suggesting that the pairing involves either multiple bands or multiple order parameters. To examine these issues, we have used Andreev reflection spectroscopy, performed with ballistic point contacts over a range of temperatures and magnetic fields. We observed distinct spectral evidence for gap nodes. We also observed multiple spectral features arising from Ru-doping. We interpret the evolution of these spectral features within the scenario of multigap pairing.

1. Introduction

The discovery of superconductivity in the heavy-fermion filled skutterudite compound PrOs₄Sb₁₂¹ has attracted much interest, particularly because of its unconventional properties. A double superconducting transition at $T_{c1} \sim 1.8$ K and $T_{c2} \sim 1.7$ K has been observed^{2–4} suggesting that there may be multiple superconducting phases. Different experiments have reported different field-vs-temperature ($H - T$) phase diagrams. For example, angular magneto-thermal-conductivity $\kappa(H, \phi)$ data indicates that a superconducting order parameter (OP) undergoes a field-induced phase transition from two point nodes at low fields, to six point nodes at high fields.⁵ However, specific heat^{6–8} and ac magnetic susceptibility χ measurements⁷ have not observed this transition.

Despite numerous experimental and theoretical studies, the superconducting gap topology of PrOs₄Sb₁₂ has still not been established. Penetration depth,⁹ $\kappa(H, \phi)$,⁵ small angle neutron scattering¹⁰ and specific heat $C(T)$ ¹¹ experiments have all indicated the presence of gap nodes. In contrast, muon-spin resonance,¹² Sb-nuclear quadrupolar resonance,¹³ scanning tunnelling spectroscopy¹⁴ and $\kappa(T, H)$ ¹⁵ measurements have shown the Fermi surface to be fully gapped in the superconducting state. PrOs₄Sb₁₂ has a complex Fermi topology with multiple sheets on the Fermi surface,¹⁶ and recent $\kappa(T, H)$ measurements have indicated that it is a multiband superconductor.¹⁵ The discrepancy between experiments that see gap nodes and those that do not, can be explained by a scenario where a nodal gap exists on the small-mass band and the large-mass band is fully gapped.¹⁷ Recent $C(T)$ measurements on Pr(Os_{1-x}Ru_x)₄Sb₁₂ showing fully gapped behaviour for x as low as 0.01 would be consistent with this picture.¹¹ However, direct evidence for co-existing gaps with different symmetries is still lacking.

Point-contact spectroscopy (PCS) is a powerful technique for studying unconventional superconductors, as it is a microscopic probe of both the amplitude and phase of the OP. It has been used to reveal evidence for multi-

band superconductivity in MgB₂¹⁸ and CeCoIn₅.¹⁹ Andreev reflection (AR) and quasiparticle tunnelling are the two main processes responsible for the conductance dI/dV spectrum seen in a normal-metal/superconductor junction. For conventional s -wave superconductors the primary contribution to the dI/dV in high transparency junctions is AR, the process by which a normal current is converted to a supercurrent.²⁰ These Andreev *bulk* states cause a hump-like feature in the dI/dV spectrum resulting in *excess* spectral area. For superconductors with gap nodes, due to a sign change in the OP at the node, constructive interference between consecutively reflected quasi-particles results in Andreev *surface* states. These *surface* states manifest themselves in the dI/dV spectrum as a peak at zero-bias accompanied by dips at higher energy.^{21–23} The area of the dips and peak are equal thus *conserving* total spectral area.

2. Experimental

Andreev Spectroscopy measurements were made using etched Pt-Ir tips to form ballistic²⁴ point contacts on the c -axis faces of Pr(Os_{1-x}Ru_x)₄Sb₁₂ crystals for $x = 0$ and $x = 0.02$. For low Ru-doping, the effective electron mass remains enhanced²⁵ and Andreev spectroscopy is ideally suited to examine if a gapped OP component develops at such doping levels. The measurements were made in a ³He-⁴He dilution refrigerator, down to 80 mK and up to 2.5 T. The applied magnetic field was oriented perpendicular to the c -axis faces of the crystals. Junction impedances were typically $\sim 0.2 - 1 \Omega$. Current versus voltage ($I-V$) curves were obtained by current biasing the sample using a 4-lead configuration. To minimize Joule heating a pulsed technique was employed. Pulse lengths of 2 ms with a 20% duty cycle were used and the voltage was measured 80 times during each pulse and averaged. The resulting $I-V$ curves were numerically differentiated to obtain the dI/dV spectra as a function of V .

Single crystal samples of Pr(Os_{1-x}Ru_x)₄Sb₁₂ were grown with a molten-metal-flux method.²⁶ Before measurements, to remove any excess Sb flux, the samples were etched in a 1:1 HNO₃-HCl mixture and rinsed in

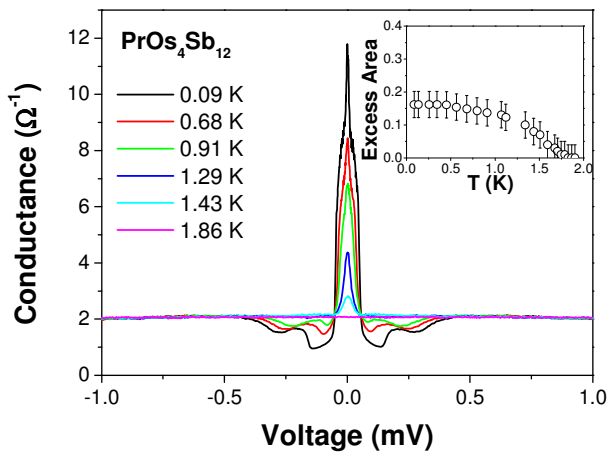


Fig. 1. Temperature dependence of the conductance spectrum for a Pt-Ir/PrOs₄Sb₁₂ point-contact junction. Decreasing zero-bias conductance peak height corresponds to increasing temperature. Shown in the inset is the evolution of the excess spectral area (arbitrary units) with temperature.

ethanol. Samples etched in this way showed the most reproducible spectra. Electrical resistivity $\rho(T, H)$ was measured with an AC resistance bridge using ultra-low current modulation. For the $x = 0$ sample a sharp superconducting transition at $T_c \sim 1.87$ K was observed in zero field and at base temperature it was found that the upper critical field $H_{c2} \sim 2.25$ T. $\chi(T)$ measurements were also performed for the $x = 0$ sample and showed a double superconducting transition at $T_{c1} \sim 1.85$ K and $T_{c2} \sim 1.7$ K.

3. Discussion

Figure 1 shows the temperature evolution of point-contact dI/dV data taken on a $x = 0$ sample in zero magnetic field. At 90 mK there is a pronounced zero-bias conductance peak (ZBCP) accompanied by symmetric dips located at $\sim \pm 0.4$ mV. There are also additional satellite features at $\sim \pm 0.3$ mV and $\sim \pm 0.2$ mV. As the temperature is increased the dips and satellite features move inward and the height of the ZBCP decreases. The dI/dV flattens out above $T \sim 1.8$ K. Shown in the inset is the excess spectral area, which was calculated by subtracting the normal-state conductance from each spectrum and then numerically integrating between ± 1.8 mV. As the temperature is lowered, the excess spectral area increases.

The presence of the ZBCP provides spectroscopic evidence for nodes in the superconducting OP. Recent theoretical work has calculated the dI/dV spectra for various spin singlet and spin triplet OP's proposed for PrOs₄Sb₁₂.²⁷ The dI/dV for one of the candidate spin triplet pair potentials with point nodes shows a ZBCP and satellite features resembling those seen in Figure 1.

Figure 2 shows the temperature evolution of the dI/dV spectrum for a $x = 0.02$ sample. At 90 mK there is a ZBCP, but its height is smaller than the one seen in the $x = 0$ sample. Additional broad hump-like features are also observed at $\sim \pm 0.6$ mV and $\sim \pm 1.4$ mV. As the temperature is increased both of these features become

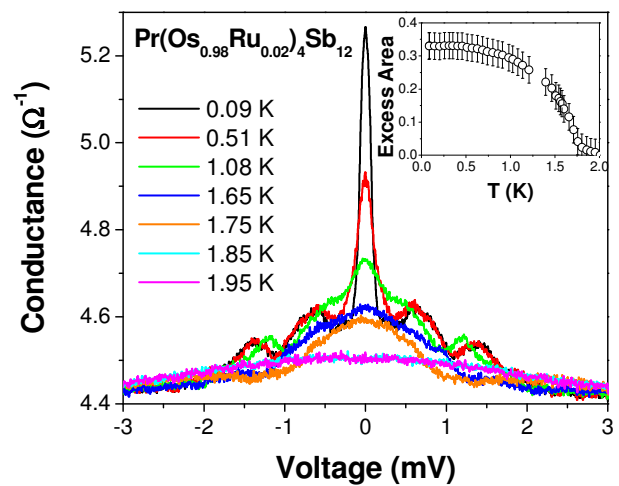


Fig. 2. Temperature dependence of the conductance spectrum for a Pt-Ir/Pr(Os_{0.98}Ru_{0.02})₄Sb₁₂ point-contact junction. Decreasing zero-bias conductance peak height corresponds to increasing temperature. Shown in the inset is the evolution of the excess spectral area (arbitrary units) with temperature.

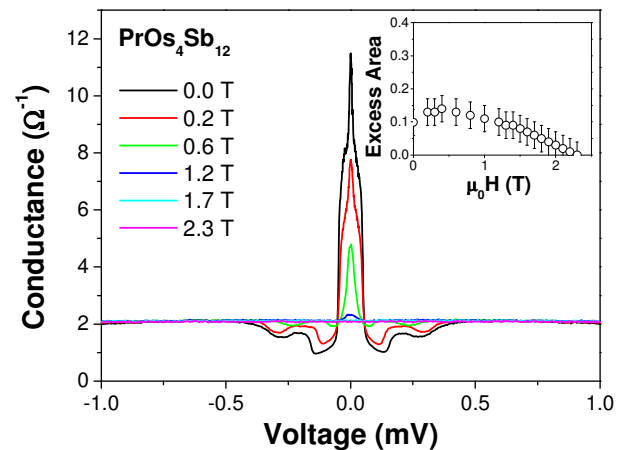


Fig. 3. Magnetic field dependence of the conductance spectrum for a Pt-Ir/PrOs₄Sb₁₂ point-contact junction at 80 mK. Decreasing zero-bias conductance peak height corresponds to increasing field. Shown in the inset is the field dependence of the excess spectral area (arbitrary units).

less broad and the ZBCP height decreases, eventually disappearing at $T \sim 1.8$ K. Shown in the inset is the temperature dependence of the excess spectral area. As the temperature is lowered the excess spectral area increases.

Figure 3 shows the magnetic field evolution of the dI/dV spectrum taken on a $x = 0$ sample at base temperature. As the field is increased the ZBCP height decreases and the dips and satellite features move inward. The ZBCP peak vanishes at ~ 1.5 T, which is lower than $H_{c2} \sim 2.25$ T, as determined by $\rho(T, H)$. The inset shows the magnetic field evolution of the excess spectral area. As the field is lowered the excess spectral area increases.

Figure 4 shows the magnetic field evolution of the dI/dV spectrum for a $x = 0.02$ sample at 80 mK. The hump-like features become less broad and the ZBCP

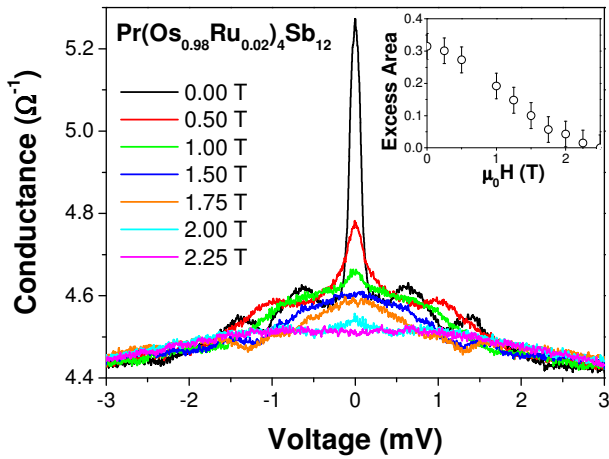


Fig. 4. Magnetic field dependence of conductance spectrum for a Pt-Ir/Pr(Os_{0.98}Ru_{0.02})₄Sb₁₂ point-contact junction at 80 mK. Decreasing zero-bias conductance peak height corresponds to increasing field. Shown in the inset is the field evolution of the excess spectral area (arbitrary units).

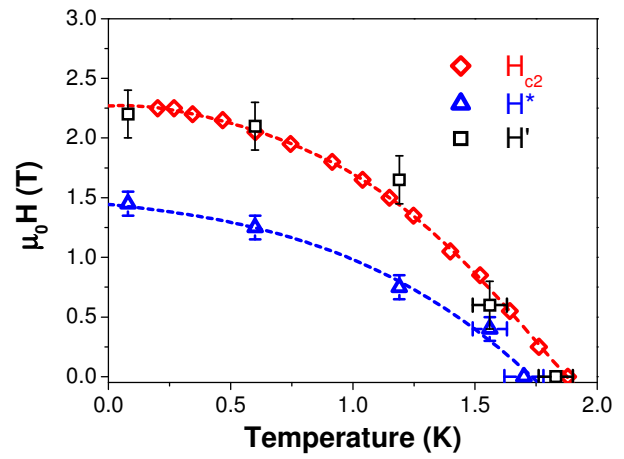


Fig. 5. $H - T$ phase diagram as determined from resistivity and point-contact spectroscopy measurements. H_{c2} (diamonds) corresponds to $\rho(T, H)$ data. H^* (triangles) corresponds to the field at which the ZBCP vanishes and H' (squares) corresponds to the field above which no excess spectral area exists. Dashed lines are a guide to the eye.

height decreases as the field is increased. However, unlike the $x = 0$ case, above 1.5 T a broad hump-like feature can still be seen up to ~ 2.2 T. Shown in the inset is the field dependence of the excess spectral area. As the field is lowered the excess spectral area increases.

Ru-doping appears to have a pronounced effect on the dI/dV spectrum. For $x = 0$, a large ZBCP indicates that Andreev *surface* states are mainly contributing to the dI/dV . For $x = 0.02$, the emergence of broad hump-like features in the dI/dV suggest that at this doping level Andreev *bulk* states play a much larger role in the dI/dV spectrum compared to $x = 0$. Our results are qualitatively consistent with $C(T)$ measurements which show a fully gapped OP component for doping as low as $x = 0.01$.¹¹

It is worth noting that, for $x = 0$, the excess spectral area increases as the temperature is lowered below T_c . Andreev *surface* states by themselves can not account for this excess as they should be conserved. Since excess area arise from Andreev *bulk* states, this temperature evolution indicates that an OP component in addition to the one responsible for the ZBCP contributes to the dI/dV . Our results therefore provide spectroscopic evidence for multiple OP components existing in PrOs₄Sb₁₂.

Two separate $\kappa(T, H)$ studies have indicated that PrOs₄Sb₁₂ is a multiband superconductor.^{15, 28} However, one of these studies suggested that the superconducting OP is fully gapped on both bands,¹⁵ whereas the other indicated that while one OP component is fully gapped (large-mass band) the other OP component is nodal (small-mass band).²⁸ Our spectroscopic results, which also indicate the presence of a nodal OP component, are consistent with the multiband and multi-symmetry scenario proposed in Ref [28].

The spectral evolution of the $x = 0$ case is also remarkable. On applying a magnetic field, the excess spectral area decreases. Above 1.5 T the ZBCP is no longer visible in the dI/dV yet excess states persist to ~ 2.2 T, suggesting that in this field range only one OP component

is contributing to the dI/dV . Our results are qualitatively similar with $\kappa(H, \phi)$ measurements which reported a field-induced change in the superconducting OP.⁵

The magnetic field levels above which the ZBCP is no longer discernible and up to which the excess spectral area persists has been tracked as a function of temperature. Figure 5 shows the resulting $H - T$ phase diagram. Defining H^* as the field at which the ZBCP vanishes, it can be seen that $H_{c2}(T)$, as determined by $\rho(T, H)$, and $H^*(T)$ emerge from distinct low-temperature asymptotes and appear to gradually approach each other as temperature is increased. Defining H' as the field up to which excess spectral area persists (indicated by squares in Figure 5) it can be seen that the $H'(T)$ and $H_{c2}(T)$ points coincide. Above H_{c2} the sample is no longer superconducting and so the amplitude of all OP components is zero. As the $H'(T)$ and $H_{c2}(T)$ curves overlap each other, it indicates that the OP component responsible for the excess states in the dI/dV persists up to H_{c2} . The behaviour of $H'(T)$ should be contrasted with that of the OP component responsible for the ZBCP which appears to only persist up to H^* .

Between $H^*(T)$ and $H_{c2}(T)$ the dI/dV spectra should reflect the OP symmetry. Theoretical dI/dV spectra have been calculated for various high-temperature OPs proposed for PrOs₄Sb₁₂, and some of these spectra show virtually no dependence on bias voltage,²⁷ consistent with our data above the H^* curve. While it is difficult to determine the exact OP symmetry in this high-field region, from the excess spectral area observed, we can nonetheless infer that an OP component persists up to H_{c2} .

$H^*(T)$ and $H_{c2}(T)$ appear to converge to different temperatures at $H = 0$ T. Since a double superconducting transition for the $x = 0$ sample was seen in $\chi(T)$ it is interesting to consider whether $H_{c2}(T)$ converges to $T_{c1} \sim 1.85$ K and $H^*(T)$ converges to $T_{c2} \sim 1.7$ K. Due to the close proximity of T_{c1} and T_{c2} , however, it is diffi-

cult to definitively determine whether or not the $H^*(T)$ and $H_{c2}(T)$ curves do indeed terminate at different T_c . Furthermore, it has not been resolved whether the double superconducting transition is intrinsic. $\kappa(T, H)$ has shown evidence for multiband superconductivity in samples exhibiting a single T_c .¹⁵ It would be interesting to spectroscopically track $H^*(T)$ and $H_{c2}(T)$ in such single T_c samples and compare the low-temperature and low-field asymptotes with those observed for samples exhibiting a double T_c .

Ru-doping has a dramatic effect on the superconducting OP in $\text{Pr}(\text{Os}_{1-x}\text{Ru}_x)_4\text{Sb}_{12}$. Our data indicates that for $x = 0$ there are multiple OP components, one of which is nodal. The fully Ru-doped compound $\text{PrRu}_4\text{Sb}_{12}$ on the other hand has been reported as having a fully gapped superconducting OP.^{29,30} As Andreev spectroscopy is a phase sensitive local probe, it is ideally suited to examine how the OP evolves from $x = 0$ to $x = 1$. The effect of Ru-doping on the two OP-components observed in $\text{PrOs}_4\text{Sb}_{12}$ can be determined by obtaining a $H - T$ phase diagram at various doping levels and observing how the nodal OP component (H^*) is suppressed as doping is increased.

4. Conclusions

Point-contact spectroscopy measurements were performed on $\text{Pr}(\text{Os}_{1-x}\text{Ru}_x)_4\text{Sb}_{12}$ crystals for $x = 0$ and $x = 0.02$. For $x = 0$ a pronounced ZBCP was observed in the dI/dV indicating the presence of a nodal OP component. For $x = 0.02$ additional hump-like features were seen in the dI/dV below T_c and H_{c2} . Excess spectral area was observed at low temperatures for both $x = 0$ and $x = 0.02$, consistent with the presence of multiple OP components with different symmetries.

Acknowledgment

This work was supported by NSERC, CFI/OIT and the Canadian Institute for Advanced Research. The preparation of the $\text{PrOs}_4\text{Sb}_{12}$ single crystal specimens was funded by the U. S. Department of Energy under Grant No. DE-FG02-04ER46105.

- 1) E. D. Bauer, N. A. Frederick, P.-C. Ho, V. S. Zapf, and M. B. Maple: Phys. Rev B **65** (2002) 100506(R).
- 2) M. B. Maple, P.-C. Ho, V. S. Zapf, N. A. Frederick, E. D. Bauer, W. M. Yuhasz, F. M. Woodward and J. W. Lynn: J. Phys. Soc. Jpn. **71** (2002) Suppl. 23.
- 3) R. Vollmer, A. Fait, C. Pfeleiderer, H. v. Lhneysen, E. D. Bauer, P.-C. Ho, V. Zapf, and M. B. Maple: Phys. Rev. Lett. **90** (2003) 057001.
- 4) Takashi Tayama, Toshiro Sakakibara, Hitoshi Sugawara, Yuji Aoki and Hideyuki Sato: J. Phys. Soc. Jpn. **72** (2003) 1516.
- 5) K. Izawa, Y. Nakajima, J. Goryo, Y. Matsuda, S. Osaki, H. Sugawara, H. Sato, P. Thalmeier, and K. Maki: Phys. Rev. Lett. **90** (2003) 117001.
- 6) M.-A. Measson, D. Braithwaite, J. Flouquet, G. Seyfarth, J. P. Brison, E. Lhotel, C. Paulsen, H. Sugawara, and H. Sato: Phys. Rev. B **70** (2004) 064516.
- 7) K. Grube, S. Drobnik, C. Pfeleiderer, H. v. Lhneysen, E. D. Bauer, and M. B. Maple: Phys. Rev. B **73** (2006) 104503.
- 8) Toshiro Sakakibara, Atsushi Yamada, Jeroen Custers, Kazuhiro Yano, Takashi Tayama, Hidekazu Aoki, and Kazushige Machida: J. Phys. Soc. Jpn. **76** (2007) 051004.
- 9) Elbert E. Chia, M. B. Salamon, H. Sugawara, and H. Sato: Phys. Rev. Lett. **91** (2003) 247003.
- 10) A. D. Huxley, M.-A. Measson, K. Izawa, C. D. Dewhurst, R. Cubitt, B. Grenier, H. Sugawara, J. Flouquet, Y. Matsuda, and H. Sato: Phys. Rev. Lett. **93** (2004) 187005.
- 11) N.A. Frederick, T.A. Sayles, S.K. Kim and M.B. Maple: J. Low Temp. Phys. **147** (2007) 321.
- 12) D. E. MacLaughlin, J. E. Sonier, R. H. Heffner, O. O. Bernal, Ben-Li Young, M. S. Rose, G. D. Morris, E. D. Bauer, T. D. Do, and M. B. Maple: Phys. Rev. Lett. **89** (2002) 157001.
- 13) H. Kotegawa, M. Yogi, Y. Imamura, Y. Kawasaki, G.-q. Zheng, Y. Kitaoka, S. Ohsaki, H. Sugawara, Y. Aoki, and H. Sato: Phys. Rev. Lett. **90** (2003) 027001.
- 14) H. Suderow, S. Vieira, J. D. Strand, S. Budko, and P. C. Canfield: Phys. Rev. B **69** (2004) 060504.
- 15) G. Seyfarth, J. P. Brison, M.-A. Masson, D. Braithwaite, G. Lapertot, and J. Flouquet: Phys. Rev. Lett. **97** (2006) 236403.
- 16) H. Sugawara, S. Osaki, S. R. Saha, Y. Aoki, H. Sato, Y. Inada, H. Shishido, R. Settai, Y. Onuki, H. Harima, and K. Oikawa: Phys. Rev. B **66** (2002) 220504.
- 17) D. E. MacLaughlin, Lei Shu, R. H. Heffner, J.E. Sonier, F. D. Callaghan, G. D. Morris, O. O. Bernal, W. M. Yuhasz, N. A. Frederick and M. B. Maple: cond-mat/0706.0439 (2007).
- 18) P. Szabo, P. Samuely, J. Kacmarcik, T. Klein, J. Marcus, D. Fruchart, S. Miraglia, C. Marcenat and A. G. Jansen: Phys. Rev. Lett. **87** (2001) 137005.
- 19) P. M. Rourke, M. A. Tanatar, C. S. Turel, J. Berdeklis, C. Petrovic, and J. Y. T. Wei: Phys. Rev. Lett. **94** (2005) 107005.
- 20) G. E. Blonder, M. Tinkham and T. M. Klapwijk: Phys. Rev B **25** (1982) 4515.
- 21) Chia-Ren Hu: Phys. Rev. Lett. **72** (1994) 1526.
- 22) Yukio Tanaka and Satoshi Kashiwaya: Phys. Rev. Lett. **74** (1995) 3451.
- 23) M. Fogelstrm, D. Rainer, and J. A. Sauls: Phys. Rev. Lett. **79** (1997) 281.
- 24) Using the Sharvin formula, $R = 4\rho l/3\pi a^2$, with $\rho \sim 2 \mu\Omega$ cm, the mean free path, $l \sim 3500 \text{ \AA}$, and R the junction resistance, the Sharvin radius a is estimated to be ~ 140 nm thus satisfying the ballistic criterion $a < l$.
- 25) N. A. Frederick, T. A. Sayles and M. B. Maple: Phys. Rev. B **71** (2005) 064508.
- 26) N. A. Frederick, T. D. Do, P.-C. Ho, N. P. Butch, V. S. Zapf and M. B. Maple: Phys. Rev. B **69** (2004) 024523.
- 27) Yasuhiro Asano, Yukio Tanaka, Yuji Matsuda, and Satoshi Kashiwaya: Phys. Rev. B **68** (2003) 184506.
- 28) R. W. Hill, Shiyun Li, M. B. Maple and Louis Taillefer: cond-mat/0709.4265 (2007).
- 29) E.E.M. Chia, D. Vandervelde, M.B. Salamon, D. Kikuchi, H. Sugawara and H. Sato: J. Phys: Cond. Mat. **17** (2003) L303.
- 30) M. Yogi, H. Kotegawa, Y. Imamura, G.-q. Zheng, Y. Kitaoka, H. Sugawara and H. Sato: Phys. Rev. B **67** (2003) 180501.